

Co@CoO@Au core-multi-shell nanocrystals

Stephanie H. Johnson,^a Craig L. Johnson,^a Steven J. May,^{ac} Samuel Hirsch,^b M. W. Cole^b and Jonathan E. Spanier^a

Received 21st September 2009, Accepted 27th October 2009

First published as an Advance Article on the web 17th November 2009

DOI: 10.1039/b919610b

We report on the chemical synthesis, structural and compositional characterization, and hierarchical organization of Co-core, concentric CoO–Au multi-shell nanocrystals (Co@CoO@Au). Based on electron microscopy, magnetometry and spectroscopy experiments, we present compelling evidence for the formation of the Au outer shell on CoO, challenging the common assumption that the reduction reaction to form Au shells can only occur if the cobalt surface has not oxidized. Our findings suggest that the presence of a metal shell surrounding a transition-metal core nanocrystal following such a reduction reaction cannot be taken as evidence that the transition metal oxide is absent from the surface of the nanocrystal core. We find that Au shell growth can produce Co@CoO@Au nanocrystals possessing five-fold twinning symmetry and we suggest that their growth is facilitated through self nucleation and coalescence of Au particles.

Introduction

The synthesis and technological application of magnetic nanoparticles presents challenges resulting from their tendency to agglomerate and their instability in air. These difficulties commonly arise in ferromagnetic (FM) Co nanoparticles, which oxidize to form antiferromagnetic (AFM) face-centered-cubic CoO. When the surface of the Co oxidizes to create an AFM shell around the ferromagnetic Co, an exchange bias is observed due to the exchange coupling between the AFM and FM spins along the interface.^{1,2} In previous work, an oxide layer was reported to have evolved or was introduced as a protecting layer to preserve the magnetic properties of the Co core. However, even with an oxide layer the Co cores are not stable against further oxidation over time.^{3,4}

Noble-metal shells can improve the stability of transition-metal nanoparticles against oxidation. These nano-shells contribute their chemical functionality and unique surface plasmonic-resonant (SPR)-driven optical properties. These characteristics permit nanoparticle systems possessing Au nanoshells to play increasingly significant roles in new electronic and photonic devices. Furthermore, core-shell systems have important applications in biochemistry, radiology, and other medical therapies.^{5,6} Specifically, chemically inert, multi-functional monodisperse nanoparticles

exhibiting size-dependent properties such as those presented herein hold significant promise for a diverse number of applications, *e.g.* in electronic, optical and magnetic devices,⁴ and in magnetic field-assisted delivery of biomolecules and SPR-derived heating and treatment of tumors.⁶

Several strategies have been reported for producing Co@Au nanocrystals using well-known synthesis methods. For example, Dinega and Bawendi⁷ reported on the synthesis of Co seed nanocrystals *via* thermal decomposition of cobalt carbonyl. This method can yield particles averaging 20 nm in diameter and the diameter of the product can be altered by varying the types of surfactants used and their concentrations.^{7,8} Bao and co-workers prepared 5 nm and 10 nm Co seed particles by selecting different amine groups.^{9,10} In both cases, Au shells on Co nanocrystal cores were obtained through a reduction reaction on the Co surface atoms, which can serve as nucleation sites for the Au ions. The reduction reaction was carried out by injecting Au stock solution into a refluxing Co seed solution^{9–11} or by injecting the Co seed solution into a refluxing Au stock solution.¹² Some of these reports show magnetic data which suggest the presence of oxidized Co. However, the formation of cobalt oxide prior to Au shell formation was ruled out, because Au ions would not be expected to form the Au shell on an oxidized surface.^{12,13} Here we show an AFM CoO layer between the Co core and Au shell is obtained using the established gold reduction method. The presence of the Au shell is confirmed with TEM images and absorption spectroscopy and the CoO layer is observed through TEM and STEM imaging, magnetic measurements, and Raman scattering spectroscopy. We also propose a plausible mechanism for the formation of an Au shell on the Co@CoO nanocrystal surface.

Experimental

Co seed nanocrystals were synthesized by adapting established methods to include a more amine-rich surfactant which encourages Au collection on the cobalt surface.^{4,7–12} The modified Co seed synthesis followed the LaMer mechanism¹⁴ of direct injection of a metal stock solution into a refluxing surfactant solution to induce nucleation. In a typical reaction, the surfactant solution (0.35 g trioctylphosphine oxide, 0.3 mL oleic acid, and 13 mL of tri-*n*-octylamine) was refluxed at 190 °C for 15 min. The Co stock solution, (0.80 g Co-carbonyl and 4 mL tri-*n*-octylamine) was rapidly injected into the surfactant mixture facilitating the rapid decomposition of Co-carbonyl to form surfactant stabilized magnetic Co nanocrystals. Methanol was added to separate the Co nanocrystals, and the solid Co nanocrystals were re-dispersed in chloroform for characterization. This method yields mono-disperse Co seed nanocrystals approximately 10.5 nm in diameter, as seen in Fig. 2a.

^aDepartment of Materials Science & Engineering, Drexel University, Philadelphia, PA, USA

^bU.S. Army Research Laboratory, Aberdeen Proving Ground, MD, USA

^cMaterials Science Division, Argonne National Laboratory, Argonne, IL, USA

The synthesis of the Au shell on the Co core followed the established method of Au reduction on the surface of the Co seed.⁹⁻¹² This process begins by refluxing 0.75 g of the Co nanocrystal solids in 5 mL of toluene in the reaction vessel for 15 min at 85 °C. Next, an Au stock solution is made up of 0.0185 g hydrogen tetrachloroaurate(III) hydrate, 3 mL toluene, and 0.5 mL oleylamine. The Au solution is rapidly injected into the refluxing Co nanocrystal solution and allowed to react for one hour. The multi-component nanocrystal product was separated from the Au nanocrystals using magnetic separation. The samples were then rinsed and re-dispersed in solvent for characterization, yielding mono-disperse core-shell nanocrystals approximately 14.5 nm ± 3 nm in diameter (Fig. 3a).

UV-Vis absorption spectroscopy

Samples were dispersed in chloroform and the absorption spectra were collected on a Shimadzu model UV 2501 PC spectrophotometer.

Transmission electron microscopy (TEM) and scanning TEM (STEM) measurements

Samples were prepared on a 400-mesh Cu grid with an ultra-thin carbon film (Pacific Grid Tech). TEM and high-angle annular-dark-field (HAADF) STEM analysis were collected using a JEOL 2100F with an accelerating voltage of 200 kV and equipped with a Gatan HAADF detector with a 0.2 nm probe size.

Magnetic measurements

The magnetically separated fraction of our nanocrystals were drop-cast on SiO₂-coated Si(100) wafers and zero field-cooled (ZFC) and field-cooled (FC) magnetization as a function of temperature and magnetic field were collected using a magnetic properties measurement system-superconducting quantum interference device (MPMS-SQUID, Quantum Design, San Diego, CA).

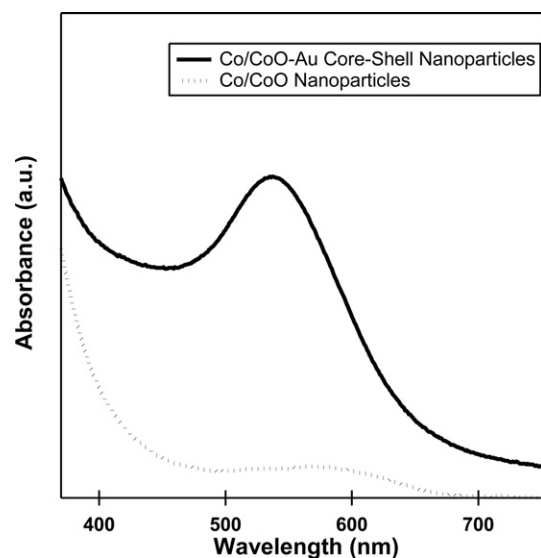


Fig. 1 The UV-Vis absorbance spectra for Co@CoO nanocrystals (···) and Co@CoO with Au shell nanocrystals (—).

Raman scattering spectroscopy

Magnetic stir-bar selected synthetic product was drop-cast on a SiO₂-coated Si(100) wafer possessing 250 nm and 50 nm thick layers of thermally evaporated Cr and Au, respectively. Raman spectra were collected at room temperature using the 514 nm line of an Ar-ion laser as excitation.

Results and discussion

Fig. 1 shows the optical absorption spectrum for the Co@CoO seed nanocrystals (dotted line) and the Co@CoO@Au core-shell particles (solid line). The addition of the Au shell is seen to produce an absorbance peak near 550 nm. The wavelength of this peak, which is

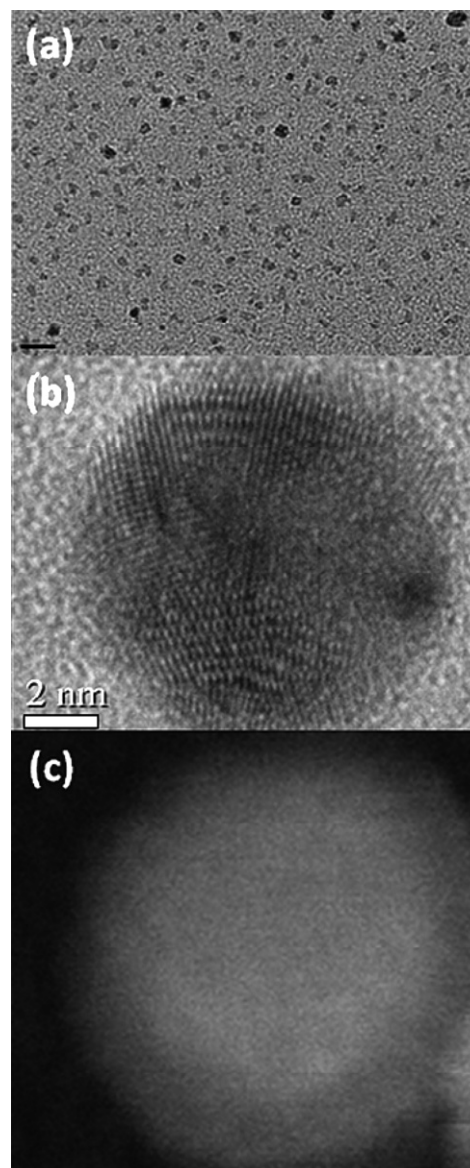


Fig. 2 TEM and STEM images of Co@CoO nanocrystals. (a) A TEM image of Co@CoO nanocrystals, scale bar 20 nm. (b) A HR-TEM image of a Co@CoO nanocrystal, showing the overlapping crystal orientations of the Co and CoO (scale bar 2 nm). (c) A HAADF image showing the bright Co core and darker CoO shell.

due to the surface-plasmon resonance of the Au shell, appears red-shifted compared to solid Au nanocrystals of comparable diameter with an absorption peak around 520 nm.^{10,11} This shift may be attributed to the thickness of the Au shell and the wavelength-dependent complex dielectric function contribution from the CoO–Au interface that is distinct from that for solid Au nanocrystals. This result is consistent with a report of progressive blue-shifting of the absorbance peak for a magnetic oxide core possessing increasing numbers of Au shell layers.¹⁵

Our Co nanocrystals have an average diameter of 10.5 nm (Fig. 2a). The HRTEM image of the Co@CoO nanocrystal (Fig. 2b) shows Moiré fringe interference patterns which result from overlapping crystal orientations. The presence of Moiré fringes indicate the overlapping of the Co and CoO crystal structures. We used HAADF STEM imaging to map the composition of our Co@CoO nanocrystals at the sub-nanometer scale. HAADF STEM images are generated by integrating only electrons scattered to high angles on an annular detector. These Rutherford-scattered electrons produce image contrast that is proportional to atomic number.¹⁶ In Fig. 2c the HAADF image of the Co@CoO nanocrystal shows core-shell contrast where the bright and dark areas correspond to the Co core and CoO shell, respectively, suggesting that the CoO layer forms prior to the Au shell reaction.

The TEM image of the multi-shell product indicates that the Co@CoO@Au nanocrystals are fairly monodisperse, with an average diameter around 14.5 nm (Fig. 3a). By comparing the images of the Co@CoO nanocrystals and Co@CoO@Au nanocrystals, we can conclude that the Au shell is ~2 nm thick. High resolution images

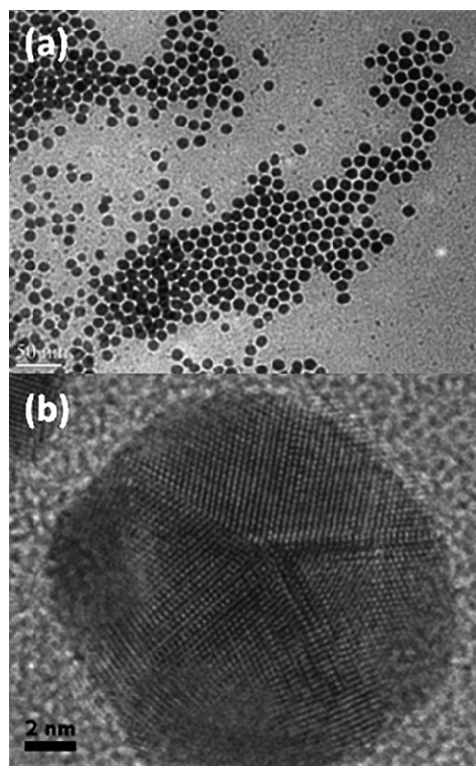


Fig. 3 TEM image of Co@CoO@Au nanocrystals. (a) TEM image displaying the monodispersity of the nanocrystals (scale bar 50 nm). (b) HR-TEM image showing Moiré fringes and five-fold twinning (scale bar 2 nm).

of these particles like the one shown in Fig. 3b reveal that the Co@CoO@Au nanocrystals exhibit five-fold symmetry characteristic of fcc-Au. Multi-twin particles can be the result of smaller particles coalescing to form a larger particle or a shell around a particle.^{17–19} Five-fold twinning is adopted by particles to reduce surface energy by orienting around the [111] plane.^{17–21} The Moiré fringe in the center of the particle (Fig. 3b) is an indication of the overlap of the Au lattice with the Co@CoO lattice and that the particle is not merely an Au nanoparticle.

Zero-field cooled (ZFC) and field cooled (FC) magnetic hysteresis measurements were collected to observe the exchange bias from the Co@CoO interface in the Co@CoO@Au nanocrystals. Magnetization measurements performed on magnetically separated nanocrystals further confirm the existence of a CoO layer between the Co core and Au shell. Magnetization data, collected at 5, 15, and 40 K after zero-field cooling, is presented in Fig. 4a. The FM hysteresis for the Co core, CoO shell (CoO@Co) nanocrystals is still observed when the sample is cooled from its Néel temperature T_N in the absence of an applied field (zero-field cooling measurement), but when a field is applied during cooling (field cooling measurement) the hysteresis is shifted along the field axis.^{3,22,23} Magnetic hysteresis is observed, confirming the presence of ferromagnetic Co within the particles. From Fig. 4b we see that hysteresis loops obtained after field cooling in 5 kOe exhibit a significant exchange bias ($H_E \approx 1$ kOe), brought on by the exchange coupling at the interface between the FM Co core and AFM CoO shell. The magnitude of the exchange bias is consistent with previous studies of Co@CoO particles.^{22,24,25} The temperature dependent FC and ZFC magnetization behavior (Fig. 4c) is also consistent with previous reports of CoO shells on Co nanocrystals.^{13,26}

Raman-scattering spectra collected from the magnetically separated product (Fig. 5) show first-order peaks, at ~469, ~511 and ~672 cm^{-1} , with mode symmetry assignments to A_{1g} , F_{2g} , and E_g , respectively. The spectra confirm the presence of oxidized cobalt in the form of CoO. Although a fourth first-order Raman-active peak possessing F_{2g} symmetry can be expected^{23,27,28} near 605 cm^{-1} for CoO, this mode is much weaker and is not discernable in our spectrum.

The growth of an Au shell on Co@CoO using the Au reduction method has not been explored before this work. While the growth mechanism still remains to be explored, we suggest a plausible growth mechanism for our Co@CoO@Au product. Reported Au shell growth reactions follow a reduction mechanism to form an Au shell, which can also allow for the self-nucleation of Au nanocrystals.^{11,12} In our synthesis, we suggest that the self-nucleated Au particles collect around the amine-rich surface of the Co@CoO particles, and then coalesce to form an Au shell surrounding the Co@CoO nanocrystal (Scheme 1).

Conclusions

In this work we demonstrate the growth of core-multi-shell Co@CoO@Au nanocrystals. Through the use of HAADF STEM imaging, shifted FC hysteresis, temperature-dependent magnetic moments, and Raman scattering spectroscopy, we confirm the presence of CoO at the interface between the Co and Au layers of these core shell particles. HRTEM images, energy-dispersive X-ray spectra, and optical absorption spectra provide evidence that these Au shells form as a result of rapid self-nucleation and coalescence of

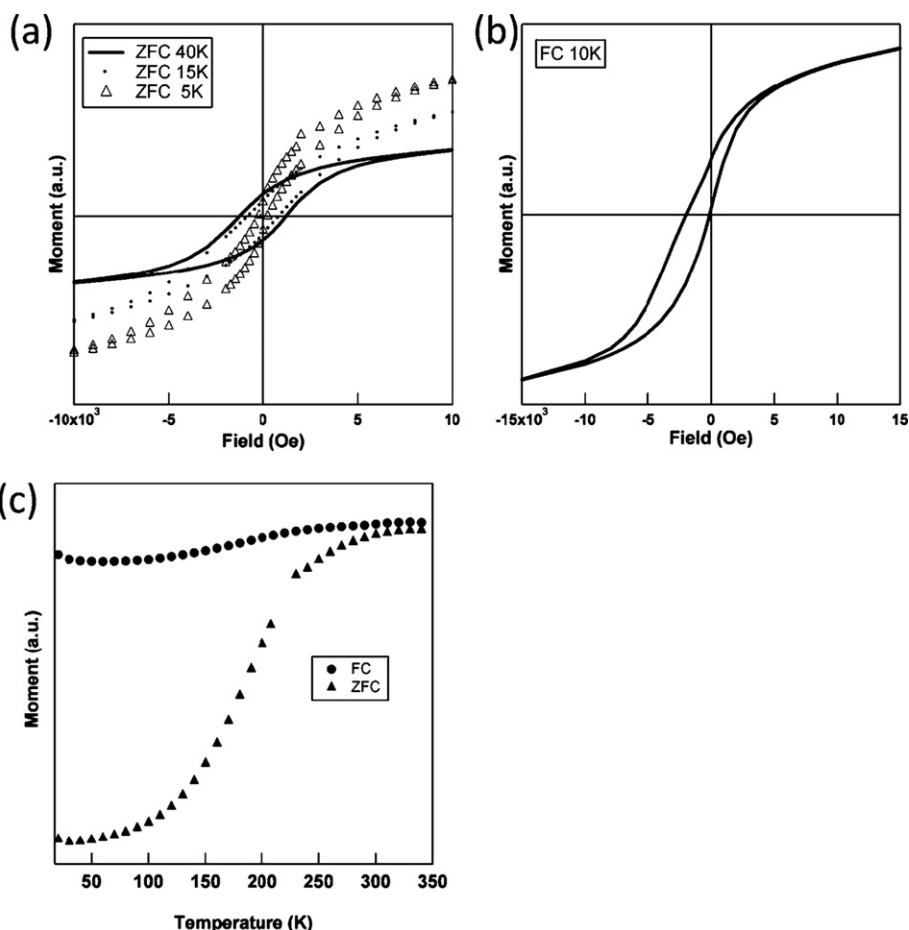


Fig. 4 (a) ZFC hysteresis of Co@CoO@Au nanocrystals measured at 40 K, 15 K, 5 K. (b) FC hysteresis for Co@CoO@Au nanocrystals measured at 10 K. (c) Field-cooled (FC) and zero-field-cooled (ZFC) magnetic moment vs. T curves of Co@CoO@Au nanocrystals at an applied field and cooling field of 100 Oe.

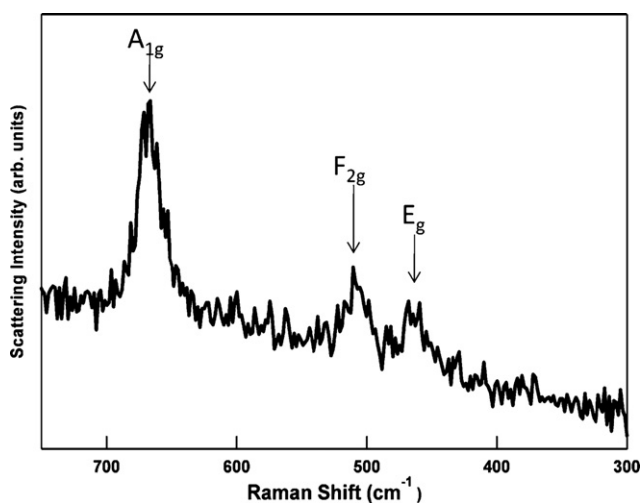
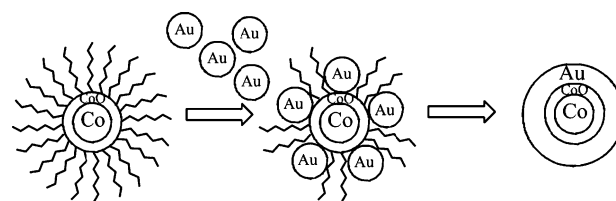


Fig. 5 Room temperature Raman scattering spectra collected from the magnetically separated Co@CoO@Au product. These peaks, at ~469, ~511 and ~672 cm⁻¹, with mode symmetry assignments to A_{1g}, F_{2g}, and E_g, respectively, confirm the presence of oxidized cobalt in the form of CoO.

the Au nanoclusters onto the Co@CoO nanocrystals. We hope these findings will stimulate further investigation of the properties of FM metal-oxide-metal core-multi-shell nanocrystals and their formation.



Scheme 1 Coalescence of Au nanocrystals on Co@CoO to form a Co@CoO@Au core-multi-shell nanocrystal.

Acknowledgements

The authors thank Peter Finkel for assistance with additional magnetic measurements and Zhorro Nikolov and Dominic Bruzzese for collecting Raman scattering spectra. We would also like to thank Fredrick Beyer for helping coordinate access to the JEOL 2100F at ARL-APG. S.H.J. is supported by a GAANN Fellowship in Material Science at Drexel University. J.E.S. gratefully acknowledges the U.S. Army Research Office for support under W911-NF-08-1-0067.

References

- 1 W. H. Meiklejohn and C. P. Bean, *Phys. Rev.*, 1957, **105**, 904.
- 2 J. Nogues, J. Sort, V. Langlais, V. Skumryev, S. Surinach, J. S. Munoz and M. D. Baro, *Phys. Rep.*, 2005, **422**, 65.

- 3 D. Srikala, V. N. Sigh, A. Banerjee, B. R. Mehta and S. Patnaik, *J. Phys. Chem. C*, 2008, **112**, 13882.
- 4 S. Sun and C. B. Murray, *J. Appl. Phys.*, 1999, **85**, 4325.
- 5 A. W. Lin, N. A. Lewinski, J. L. West, N. J. Halas and R. A. Drezek, *J. Biomed. Opt.*, 2005, **10**(6), 064035.
- 6 G. Chen, M. Takezana, N. Kawazoe and T. Tateishi, *Open Biotechnol. J.*, 2008, **2**, 152.
- 7 D. P. Dinega and M. G. Bawendi, *Angew. Chem., Int. Ed.*, 1999, **38**, 1788.
- 8 V. F. Puentes, K. M. Krishnan and A. P. Alivisatos, *Science*, 2001, **291**, 2115.
- 9 Y. Bao, A. B. Pakhomov and K. M. Krishnan, *J. Appl. Phys.*, 2005, **97**, 10J317.
- 10 Y. Bao, H. Calderon and K. M. Krishnan, *J. Phys. Chem. C*, 2007, **111**, 1941.
- 11 G. Cheng, A. R. Hight Walker and J. Magn, *J. Magn. Magn. Mater.*, 2007, **311**, 31.
- 12 S. Mandal and K. M. Krishnan, *J. Mater. Chem.*, 2007, **17**, 372.
- 13 Y. H. Xu and J. P. Wang, *IEEE Trans. Magn.*, 2007, **43**, 3109.
- 14 V. K. LaMer and R. H. Dinegar, *J. Am. Chem. Soc.*, 1950, **72**, 4847.
- 15 J. L. Lyon, D. A. Fleming, M. B. Stone, P. Schiffer and M. E. Williams, *Nano Lett.*, 2004, **4**, 719.
- 16 S. J. Pennycook, *Ultramicroscopy*, 1989, **30**, 58.
- 17 Z. R. Dai, S. Sun and Z. L. Wang, *Nano Lett.*, 2001, **1**, 443.
- 18 H. Y. Park, M. J. Schadt, L. Wang, I. I. S. Lim, P. N. Njoki, S. H. Kim, M. Y. Jang, J. Lou and C. J. Zhong, *Langmuir*, 2007, **23**, 9050.
- 19 Y. Q. Wang, W. S. Liang and C. Y. Geng, *Nanoscale Res. Lett.*, 2009, **4**, 684.
- 20 C. J. Johnson, E. Dujardin, S. A. Davis, C. J. Murphy and S. Mann, *J. Mater. Chem.*, 2002, **12**, 1765.
- 21 Y. Chen, X. Gu, C. G. Nie, Z. Y. Jiang, Z. X. Xie and C. J. Lin, *Chem. Commun.*, 2005, 4181.
- 22 I. N. Krivorotov, H. Yan, E. D. Dahlberg and A. Stein, *J. Magn. Magn. Mater.*, 2001, **226–230**, 1800.
- 23 J. B. Yi and J. Ding, *J. Magn. Magn. Mater.*, 2006, **303**, e160.
- 24 S. E. Inderhees, J. A. Borchers, K. S. Green, M. S. Kim, K. Sun, G. L. Strycker and M. C. Aronson, *Phys. Rev. Lett.*, 2008, **101**, 117202.
- 25 T. Maurer, F. Zighem, F. Ott, G. Chaboussant, G. Andre, Y. Sourmare, J. Y. Piquemal, G. Viau and C. Gatel, *Phys. Rev. B: Condens. Matter Mater. Phys.*, 2009, **80**, 064427.
- 26 G. H. Wen, R. K. Zheng, K. K. Fung and X. X. Zhang, *J. Magn. Magn. Mater.*, 2004, **270**, 407.
- 27 H. C. Choi, Y. M. Jung, I. Noda and S. B. Kim, *J. Phys. Chem. B*, 2003, **107**, 5806.
- 28 C. W. Tang, C. B. Wang and S. H. Chien, *Thermochim. Acta*, 2008, **473**, 68.